Available online at www.sciencedirect.com
ScienceDirect
Carbohydrate Research 343 (2008) 364–373
Carbohydrate RESEARCH

Heterogeneity in iota-carrageenan molecular structure: insights for polymorph II→III transition in the presence of calcium ions

Srinivas Janaswamy and Rengaswami Chandrasekaran*

Whistler Center for Carbohydrate Research, Department of Food Science, 745 Agriculture Mall Drive, Purdue University, West Lafayette, IN 47907-2009, USA

Received 29 June 2007; received in revised form 8 October 2007; accepted 24 October 2007
Available online 30 October 2007

Abstract—Iota-carrageenan is used in pharmaceutical and food applications due to its ability to complex with other hydrocolloids and proteins. Six distinct cation dependent allomorphs, consistent with its versatile functionality, have so far been observed in the solid state. In this contribution, X-ray structural details of calcium iota-carrageenan (form III) are reported. The polysaccharide retains the half-staggered, parallel, 3-fold, right-handed double helix stabilized by interchain hydrogen bonds from O–2H and O–6H in the Gal*p* units. Results show that there are four helices, rather than one in I or three in II, organized in a larger pseudo-trigonal unit cell of dimensions $a = 27.44$, $c = 13.01$ Å, and $\gamma = 120°$. The four helices have similar core structures, but their sulfate group orientations are quite different. Fifteen calcium ions and 64 water molecules hold the helices together and promote helix–helix interactions. The results portray how the helices would shuffle around in an orchestrated manner to yield calcium iota-carrageenan III from II.

Keywords: Sulfated polysaccharide; Iota-carrageenan; X-ray diffraction; Packing arrangement

1. Introduction

Marine algae contain a diverse array of polysaccharides whose functionalities include cell wall protection and energy storage apart from forming a crucial carbon source for marine bacteria.[1] Importantly, these polysaccharides offer a wide range of pharmaceutical benefits and food applications.[2,3] Their biological properties such as antitumor,[4] antitherapeutic,[5] anticoagulant,[6] and antiHIV,[7,8] to name a few, increase their usage in the development of new medicinal drugs. Among these natural resources, carrageenans have drawn the attention of food scientists due to their ability to form gels, thickeners, and possible nutritional agents. These water soluble sulfated galactans extracted from red algae *Rhodophyta* are mainly heterogeneous.[9–11] The hydrocolloids are made up of a linear galactan backbone with alternating 3-linked β-D-Gal*p* and 4-linked α-D-Gal*p*. The presence or absence of a sulfate ester at free hydroxyl positions in the disaccharide repeat results in 15 distinct types of carrageenans, to date. Only κ-, ι- and λ-carrageenans have so far been exploited industrially and subjected to extensive rheological studies for understanding their functional behavior. They contain one, two, and three sulfate groups, respectively, per disaccharide repeating unit. The gel strength decreases with increasing sulfation, while λ-carrageenan forms only viscous solutions.

Among them, ι-carrageenan [→3)-β-D-Gal*p*-4-sulfate-(1→4)-3,6-anhydro-α-D-Gal*p*-2-sulfate-(1→ repeat] has been studied in relation to its dynamical and rheological properties using techniques such as optical rotation,[12,13] NMR[14] and IR[15,16] spectroscopies, electron microscopy,[17,18] and light scattering[19–21] to understand its gelation mechanism. These studies suggest that subsequent to double helix formation, gelation is due to either salt- or temperature-induced aggregation of helices. Both monovalent and divalent cations have varying effects on gelation. Shear modulus (G') increases rapidly in the presence of divalent than monovalent ions.[22]

* Corresponding author. Tel.: +1 765 494 4923; fax: +1 765 494 7953; e-mail: chandra@purdue.edu

0008-6215/$ - see front matter © 2007 Elsevier Ltd. All rights reserved.
doi:10.1016/j.carres.2007.10.020

Divalent ions (Ca^{2+}) can even promote dimer-to-dimer transitions.[23,24] On the other hand, cooperative conformational transitions such as dissociation of dimers followed by helix-to-coil transition occur with monovalent ions (K^+).[25,26] Such results connote the effect of cations on ι-carrageenan gelation, albeit a clear mechanism of the interplay between chemical structure, cation type, and gel thermoviscoelastic properties deserves further elucidation. In this context, three-dimensional structures will aid in comprehending the physicochemical behavior. We have been working along this line of research, seeking accurate molecular structures from oriented fibers, focusing on ι-carrageenan in different salt forms.

X-ray diffraction studies on hydrated ι-carrageenan fibers have unveiled six distinct packing arrangements of akin helical structures in the presence of Na^+, K^+, Rb^+, Mg^{2+}, Ca^{2+}, and Sr^{2+} cations.[27,28] Interestingly, sodium and calcium ions alone are capable of producing three of them (I, II, and III).[28,29] These solid state motifs are in congruence with ι-carrageenan's functional versatility.[9–11] Structure analyses of Na^+ and Ca^{2+} forms have yielded accurate molecular details of secondary and tertiary interactions.[30,31] In particular, the double helix is stabilized by interchain O–6H···O-2 and O–2H···O-5 hydrogen bonds and the sulfate groups are on the surface. Helix polarity is found to have a seminal role in junction zone formation as two up (↑) and one down-pointing (↓) helices are packed in the trigonal unit cell (the non-reducing-end in the down-pointing helix is opposite to that in the up-pointing helix). The negatively charged sulfate groups actively promote stronger interhelix bridges via calcium than sodium ions. However, any change in the ester group orientations would relentlessly perturb the polymer shape as well as alter the helix–helix bridges triggering the formation of new packing arrangements, and such circumstances are evident in polymorph III (present work). Further, this study provides new insights about the polymorph II→III reorganization in oriented fibers.

2. Experimental

2.1. Fiber preparation

A solution of sodium ι-carrageenan (the purest sample available provided by FMC Corporation, USA) was prepared by dissolving 15 mg of the polysaccharide and 6 mg of NaCl in 1 mL of distilled water with constant stirring at 50 °C for 1 h. A few drops were placed in between the beaded ends of the two glass rods in a fiber puller maintaining 75% relative humidity. Oriented fibers of 3–5 mm in length were obtained after stretching the semi-dried solution for about 2 h at regular intervals. These fibers were then immersed in 0.05 M $CaCl_2$ aqueous/2-propanol solution (10:90 v/v) for about 12 weeks in the cold room (4 °C). The soaking experiments were for converting the fibers from sodium to calcium form.[28,31]

2.2. X-ray patterns and unit cell dimensions

Diffraction patterns were recorded on flat photographic films in pinhole cameras using Ni-filtered CuKα radiation ($\lambda = 1.5418$ Å). The exposure lasted up to two days and the generator was operated at 40 kV and 6 mA. A steady stream of helium gas, previously bubbled through a saturated salt solution, was continuously flushed through the specimen chamber to minimize air scattering and retain 75% relative humidity. The X-ray diffraction pattern (Fig. 1) indicates uniaxial orientation and the polycrystalline nature of the fiber. Calcite powder (characteristic spacing 3.035 Å) was used for internal calibration. Positions of the reflections were obtained by using a Stoe measuring device. These measurements were employed in calculating the pattern center, fiber rotation, and tilt and the distance (ρ) of each reflection from the reciprocal lattice origin. The relationship involving the lateral ξ and vertical ζ components of ρ is given by $\rho^2 = \xi^2 + \zeta^2$, where $\zeta = lc^*$; $\xi = a^*(h^2 + k^2 + hk)^{1/2}$ for the trigonal system. The Miller indices (h, k, l) for each reflection and reciprocal unit cell (a^*, b^*, and c^*) dimensions were estimated using in-house programs. All the 62 reflections (30 visible + 32 apparently weak) yield a trigonal unit cell with $a = 27.44$ and $c = 13.01$ Å.

2.3. Intensity data

Patterns were digitized using a Zeiss SCAI scanner with 21μ resolution. Initially images were read by IrfanView

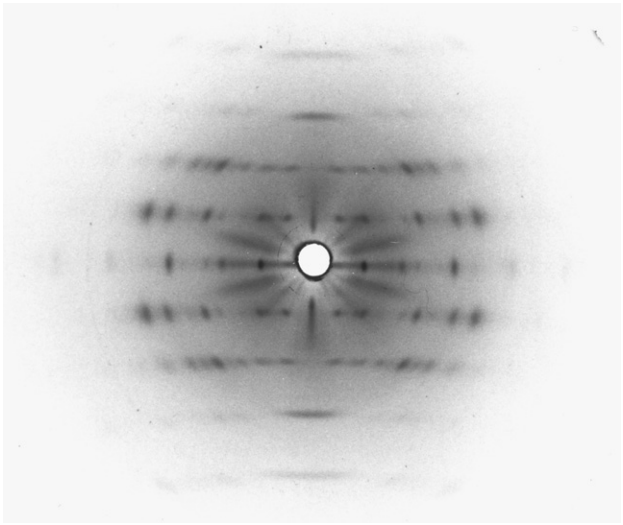

Figure 1. X-ray diffraction pattern from a well oriented and polycrystalline fiber of calcium ι-carrageenan. The Bragg reflections extend up to 2.6 Å on four layer lines. Reproduced from Ref. 28 with permission from Elsevier.

and then converted to BSL format using XCONV (http://www.ccp13.ac.uk/software/software.htm). FiberFix[32] was utilized for further processing. The background intensity was estimated by roving window methodology. Radial traces of the Bragg reflections and corresponding intensities were obtained in four quadrants from the background corrected pattern. Origin 7.5 Evaluation version (http://www.originlab.com/) was used for estimating the integrated intensity. The lowest measured intensity was assigned as the threshold value for each unobserved reflection. Lorentz and polarization corrections were applied prior to getting structure amplitudes (F_o). An unobserved reflection was included in the refinement as datum only if its calculated structure amplitude (F_c) was greater than F_o.

2.4. Molecular model and packing arrangement

A 3-fold, right-handed, half-staggered, double helix of pitch 26.02 Å (=2c) was generated using the linked-atom least-squares program (LALS).[33,34] The preferred $^4C_1$ and $^1C_4$ sugar ring conformations were used for the galactose and 3,6-anhydro galactose units, respectively. The main chain conformation angles (ϕ_1,ψ_1) and (ϕ_2,ψ_2), as well as those of the sulfate groups (θ_1, θ_2, θ_3, and θ_4) and hydroxymethyl group (χ) were refined to generate a stereochemically optimized model. The bond angles at the gycosidic bridge oxygen atoms were held at 116.5°.

The fiber density (1.69 g/mL) suggests that the unit cell has room for 12 disaccharides, corresponding to half-a-pitch of four double helices, along with 12 calcium ions and 108 water molecules. Packing analysis with (i) four up-pointing helices at (0,0), (0,1/2), (1/2,0), and (1/2,1/2), (ii) a down-pointing helix at (0,0) and three up helices at the remaining positions, (iii) three helices at (1,1/2), (1/2,0), and (1/2,1/2) related by $P3_2$ symmetry and the fourth helix at (0,0), up in one case and down in the second, and (iv) a primitive orthorhombic unit cell of half the size having $a_o = a/2$ and $b_o = \sqrt{3}a/2$, a subset of the trigonal unit cell, with two helices located at (0,0) and (1/2,1/2) either both up, or up and down, yielded high R-factor (>0.5) and incomplete solution to the structure. However, two up-pointing helices at A (0,0) and B (1/2,1/2), and two down-pointing at C (1/2,0) and D (0,1/2) in the trigonal unit cell turned out to be the best choice due to improved X-ray fit and was chosen for further analysis. For each helix, the orientation (μ) relative to the a^*-axis and translation (w) relative to the ab-plane had to be determined. Thus, setting the relative translation of helix A to zero, the 7 packing parameters (μ_A, μ_B, μ_C, μ_D, w_B, w_C, and w_D) were treated as variables. The crystallographic R-values were computed based on water-smeared scattering factors. Even though each helix maintains 3-fold screw symmetry the helices in the unit cell are not geometrically identical. Consequently, the packing symmetry reduces to $P1$ space group.

2.5. Structure refinement and guest molecules

Interhelix interactions (<4 Å) are absent at any helix orientation and translation. Hence, the packing parameters of the chosen model, μ_A to w_D, were stepped at small intervals (5° for μ and 0.05 for w) and the corresponding R-values were monitored for a possible solution. Several minima having $R \approx 0.42$ were found and tested in a series of difference electron density maps. In many cases, only a few guest molecules could be identified with little progress in the X-ray fit. However, the combination $\mu_A = 28°$, $\mu_B = 14°$, $\mu_C = 3.6°$, $\mu_D = 5.1°$, $w_B = 0.05$, $w_C = 0.06$, and $w_D = 0.06$ yielded the best possible solution. A difference electron density map showed many positive regions between the helices. Around 48 prominent peaks (as water) were selected and included one after another in the refinement. The reduction in R was monitored with the criterion that a guest molecule must be less than 3.2 Å from at least two existing oxygen atoms. Most of them survived the refinement and R dropped to 0.32. A subsequent difference electron density map, using the improved phases from the augmented structure, showed 31 more water molecules and their inclusion further reduced R to 0.24. Fifteen of these molecules able to connect with the 24 sulfate groups were re-labeled as calcium ions in the rest of the analysis. At this stage, relaxing the identity among helices provided a smaller (0.20) R. Finally, continuation of the refinement of the main chain and side group conformation angles and positions of the guest molecules improved the X-ray agreement ($R = 0.16$). The X-ray data set includes the 62 observed and 17 out of 22 unobserved reflections. A set of 708 contacts along with 79 X-ray data and 296 variables tethered to their respective expected values (total = 1083) served as observations while refining the model subject to 24 independent constraints. The resulting parameter-to-variable ratio 3.7 is comparable with other polysaccharide and polynucleotide structures solved from fiber diffraction analysis (typical values range from 3 to 11). The final model which includes 79 guest molecules has 250 additional contacts and 237 extra degrees of freedom relative to the starting model. Using this information, the observed reduction in R-value from 0.42 to 0.16 clearly establishes superiority of the final model at greater than 99.5% confidence level.[35]

3. Results

3.1. Polyanion morphology

A typical side view of the double helix is shown in Figure 2. Two interchain O–2H···O-5 and O–6H···

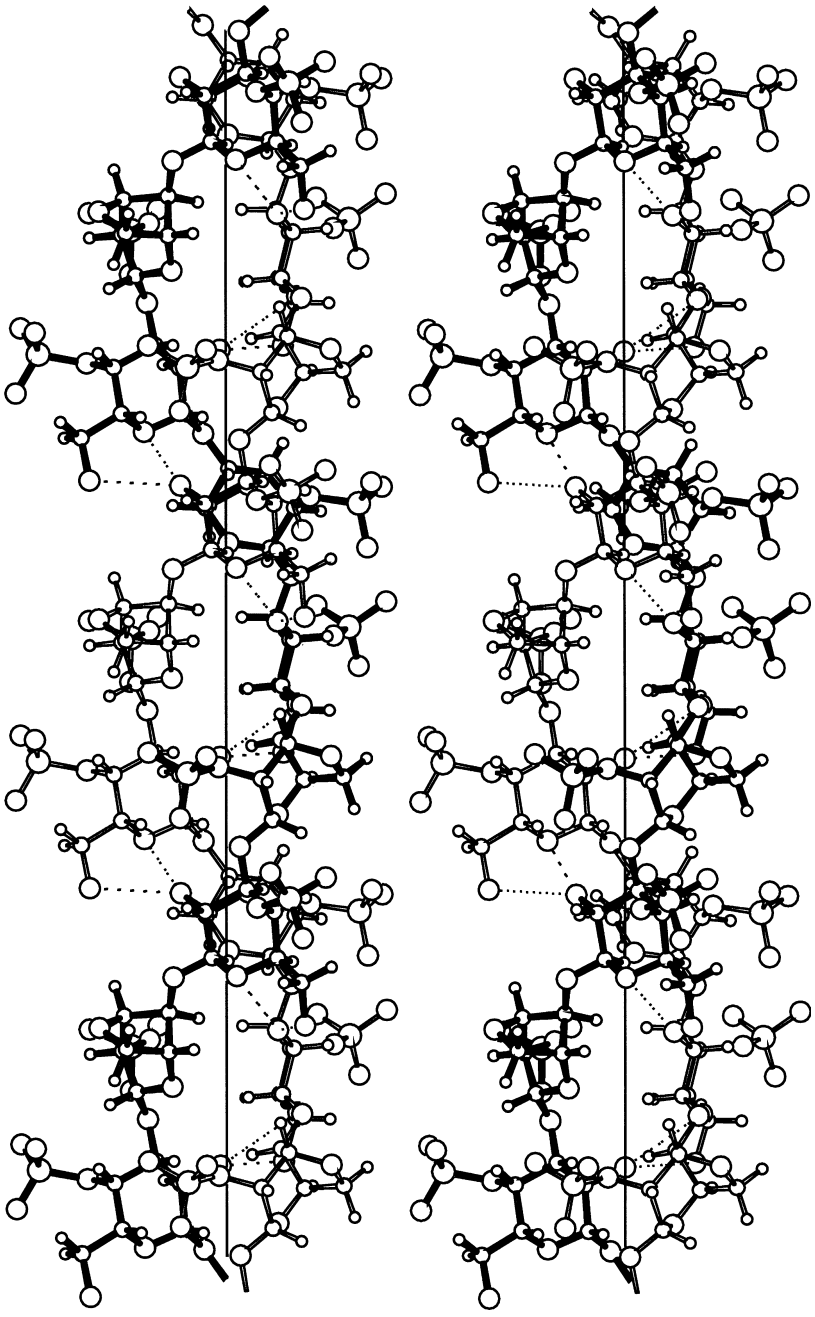

Figure 2. A stereo view of a prototype ι-carrageenan double helix of nearly one and half turns. The helix is stabilized by interchain O–2H···O-5 and O–6H···O-2 hydrogen bonds (dashed line). The vertical line is the helix axis.

O-2 hydrogen bonds are responsible for helix stabilization. The sulfate groups extend out from the helix surface. The four helices (A, B, C, and D) have similar backbone conformation angles with ϕ and ψ around −91(1)°, and 108(1)° across the 1→4 linkage and 66(1) and 76(1)° across the 1→3 linkage, respectively. These values are close to those reported for the calcium I[27] and II[31] as well as sodium[30] forms (see Table 1). The hydroxymethyl group orientation is in the same *gt* (gauche to O-5 and trans to C-4) conformation in each helix. However, a relatively significant spread exists in the sulfate group orientations. In A, B, C, and D, the 4-sulfate angles are $\theta_1 = -139$, −131, −134, and −137°, and $\theta_2 = 27°$, 29°, 34°, and 28°, respectively; the 2-sulfate angles are $\theta_3 = 106°$, 107°, 109°, and 111° and $\theta_4 = 48°$, 53°, 57°, and 55°, respectively. As a result, a marginal change in the helix diameter (13.64–13.82 Å) is noticed among the helices. This conformational heterogeneity is sufficient to affect the pattern of intra-helix bridges involving water molecules (*W*), namely, 4-*S*···*W*···2-*S* and (O-2, O-6)···*W*···2-*S*: the former type is present only in B and C, the latter is in C alone, and a third type of O-6···*W*···2-*S* bridge is seen in A, B, and D.

Table 1. Major conformation angles (in deg) in the three polymorphs of calcium ι-carrageenan helix compared with those of sodium form

Parameter	Location	III* (this study)	II (Ref. 31)	I (Ref. 27)	Sodium salt (Ref. 30)
ϕ_1 (O-5–C-1–O-4–C-4)	β-(1→4)	−91(1)	−91	−89	−87
ψ_1 (C-1–O-4–C-4–C-5)	β-(1→4)	108(1)	104	109	94
ϕ_2 (O-5–C-1–O-3–C-3)	α-(1→3)	66(1)	70	60	75
ψ_2 (C-1–O-3–C-3–C-4)	α-(1→3)	76(1)	76	77	79
χ (C-4–C-5–C-6–O-6)	Hydroxymethyl	−179(1)	176	−172	176
θ_1 (C-3–C-4–O-4–S)	4-Sulfate	−135(4)	−133	−115	−124
θ_2 (C-4–O-4–S–O–S1)	4-Sulfate	30(3)	29	32	81
θ_3 (C-1–C-2–O-2–S)	2-Sulfate	108(2)	97	99	101
θ_4 (C-2–O-2–S–O–S1)	2-Sulfate	53(4)	63	63	75

* Mean (and e.s.d.) for the four helices in the unit cell.

3.2. Calcium and water bridges

Direct interhelix hydrogen bonds are not possible because (i) the two free hydroxyl groups O–2H and O–6H are entrapped in the helix core, (ii) the helices are spaced 13.74 Å apart, close to the helix diameter, and (iii) sulfate groups between helices encounter strong electrostatic repulsion. However, calcium ions neutralize the charges and hold the surrounding helices together along with water molecules. As the helices are not related by any crystallographic symmetry, their surroundings in the entire unit cell are unrelated. The 24 sulfate groups (three 2-*S* and three 4-*S* groups per helix) in the unit cell are intricately connected by 15 calcium ions and 64 water molecules (Fig. 3). There are six 2-*S*···Ca···4-*S*, two 4-*S*···Ca···4-*S*, and one 2-*S*···Ca···2-*S* bridges between the four helices (Table 2). In addition, calcium ions curbed to either 4-*S* or 2-*S* groups are linked to nearby functional groups via water molecules. The Ca···O bond distances are similar to those observed in II[31] even though the interhelix separation has increased from 13.60 to 13.74 Å. This slight augmentation (0.14 Å) is, however, compensated by changes in sulfate group orientations (6° and 14° in 4- and 2-sulfates, respectively) and a marginal increase in helix diameter (13.64–13.82 Å).

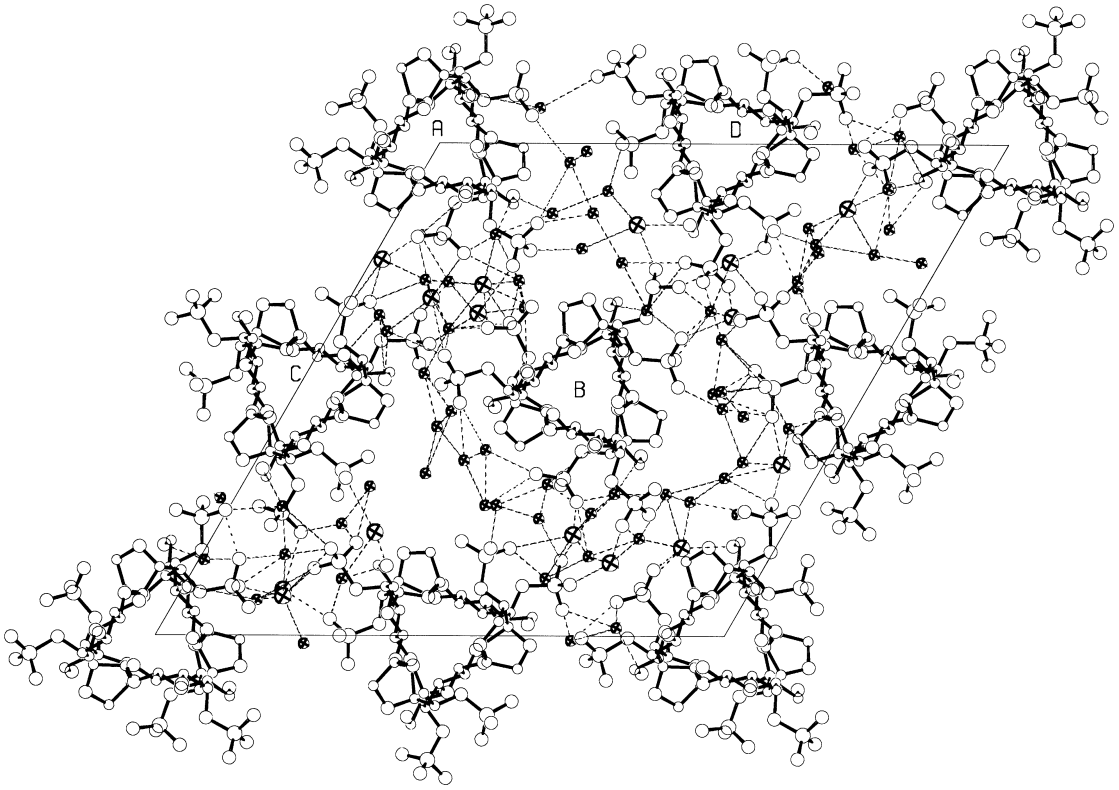

Figure 3. A projection of the unit cell down the *c*-axis. The helices A, B, C, and D are pointing up, up, down and down, respectively. Hydrogen atoms are omitted for clarity. Helices are held together by calcium (large crossed circle) ions and water (small crossed circle) molecules connected to sulfate groups.

Table 2. Attractive interactions among the ι-carrageenan helices involving calcium (Ca) ions

Interaction	Bridge	Atom X	Atom Y	X···Y (Å)	Precursor P	P–X···Y (°)
1	2-*S*···Ca···4-*S*	O–S1*B*(B,2)	Ca-1	2.71	S-*B*	139
		O–S2*A*(D,1)	Ca-1	2.49	S-*B*	147
		O–S3*A*(C,2)	Ca-2	2.44	S-*A*	143
		O–S2*A*(B,1)	Ca-2	2.79	S-*A*	147
		O–S1*B*(D,2)	Ca-2	2.43	S-*B*	138
		O–S3*B*(A,1)	Ca-5	2.92	S-*B*	143
		O–S2*A*(D,2)	Ca-5	2.62	S-*A*	105
		O–S1*B*(A,1)	Ca-6	2.89	S-*B*	105
		O–S2*B*(A,1)	Ca-6	3.17	S-*B*	93
		O–S2*A*(B,2)	Ca-6	2.88	S-*A*	137
		O–S2*A*(C,1)	Ca-12	2.94	S-*A*	111
		O–S1*B*(D,2)	Ca-12	2.66	S-*B*	138
		O–S2*B*(C,2)	Ca-14	2.95	S-*B*	124
		O–S3*A*(A,1)	Ca-14	2.61	S-*A*	161
2	4-*S*···Ca···4-*S*	O–S2*A*(B,1)	Ca-3	2.03	S-*A*	165
		O–S3*A*(D,2)	Ca-3	2.60	S-*A*	147
		O–S2*A*(A,1)	Ca-4	3.02	S-*A*	154
		O–S3*A*(C,2)	Ca-4	2.90	S-*A*	128
3	2-*S*···Ca···2-*S*	O–S1*B*(B,1)	Ca-13	2.71	S-*B*	144
		O–S1*B*(D,1)	Ca-13	3.16	S-*B*	153
4	4-*S*···Ca···*W*	O–S1*A*(B,1)	Ca-7	2.76	S-*A*	89
		O–S3*A*(B,1)	Ca-7	2.47	S-*A*	101
		O–S1*A*(A,2)	Ca-10	2.63	S-*A*	85
		O–S3*A*(A,2)	Ca-10	2.26	S-*A*	100
5	2-*S*···Ca···*W*	O–S1*B*(C,1)	Ca-8	2.63	S-*B*	94
		O–S3*B*(C,1)	Ca-8	2.67	S-*B*	92
		O–S1*B*(B,2)	Ca-9	2.59	S-*B*	78
		O–S2*B*(B,2)	Ca-9	2.92	S-*B*	67
		O–S3*B*(B,2)	Ca-9	2.30	S-*B*	89
		O–S2*B*(A,2)	Ca-11	2.88	S-*B*	95
		O–S3*B*(A,2)	Ca-11	2.81	S-*B*	98
		O–S1*B*(C,1)	Ca-15	3.44	S-*B*	88
		O–S2*B*(C,1)	Ca-15	2.98	S-*B*	108

A, B, C, and D, and 1 and 2, in parentheses after the atom name refer to the four helices in the unit cell, and the two chains in the helix. The 2- and 4-sulfate groups are indicated by 2-*S* and 4-*S*, respectively. The letters *A* and *B* designate the galactose and 3,6-anhydro galactose groups, respectively. *W* means a water molecule.

The 64 ordered water molecules (*W*) in the unit cell translate to about 5 per disaccharide repeat, compared to 4 in the calcium II[31] and 6 in the sodium[30] ι-carrageenan structures. While some of them are used for calcium mediated bridges, many others connect distant sulfate groups (*S*) by hydrogen bonding among themselves leading to a gamut of water bridges. Up to 5 *W*s are found as spacers in interactions such as *S*···*W*···*S*, *S*···*W*···*W*···*S*, *S*···*W*···*W*···*W*···*S*, *S*···*W*···*W*···*W*···*W*···*S*, and *S*···*W*···*W*···*W*···*W*···*W*···*S*. Thus, water molecules fill the gaps between helices in an orderly fashion enchancing interhelix stability. These long-range interactions also stretch out to the stashed O–6H group of the galactosyl unit. The calcium–water bridges include: ···Ca···*W*···Ca···, ···Ca···*W*···, ···Ca···*W*···*W*···, and ···Ca···*W*···*W*···*W*··· (a comprehensive list of water mediated interactions is available in the Supplementary data). These structural features underscore the importance of ordered water molecules and cations in the aggregation of ι-carrageenan helices leading to junction zones.

4. Discussion

4.1. Carrageenan assembly

Our long-term investigations on carrageenans are for obtaining precise structural details at Ångstrom level to determine their preferred interactions in the presence of cations and water molecules toward understanding their structure–function relationships. In this regard, our systematic study on ι-carrageenan has so far led to identify the structural details of polymer association in the junction zone architecture. While the nature of its 3-fold, right-handed, parallel, half-staggered double helix is independent of the cation type, there are subtle changes in helix pitch as well as notable variations in side group orientations. Apparently, these fluctuations are adequate for modulating the associative properties of helices as inferred from the existence of much larger unit cells holding up to 27 helices.[28] Such unconventional packing modes call for more than few alternatives. For example, when two or more helices pack in

a unit cell, there are, at least, three possibilities to consider: (i) identical molecular geometry, (ii) same main chain geometry but variable side group orientations, and (iii) distinct main chain as well as side group conformations. In terms of the most parsimonious solution, the first scenario is adequate for sodium[30] and calcium II[31] forms. On the other hand, only the third option is consistent with the present case (form III of calcium salt) wherein four helices with nearly similar core structures, but individually distinct side group orientations, are involved in stabilizing the packing.

Excursions from regular helix geometry as well as reduction in lattice symmetry might seem uncanny, but such circumstances are not uncommon for biopolymers. For example, hydroxymethyl group orientations in adjacent saccharides in the hydrated form of curdlan II[36] are scattered compared to the same orientation in a rigid triple helix of dehydrated curdlan III.[37] Acetamido and carboxylate group conformations in some of the hyaluronan allomorphs differ in successive repeats.[38] The carboxylate groups in the three residues of 3-fold sodium pectate helices adopt slightly different conformations.[39] Chitosan[40] and amylose A[41] and B[42] forms conform to a relaxed helical geometry. Such microconformational heterogeneities are also observed in nucleic acids. In the case of A-DNA, 11 base pairs are involved in helix stability,[43] and similarly 5 base pairs in a 2-fold helical

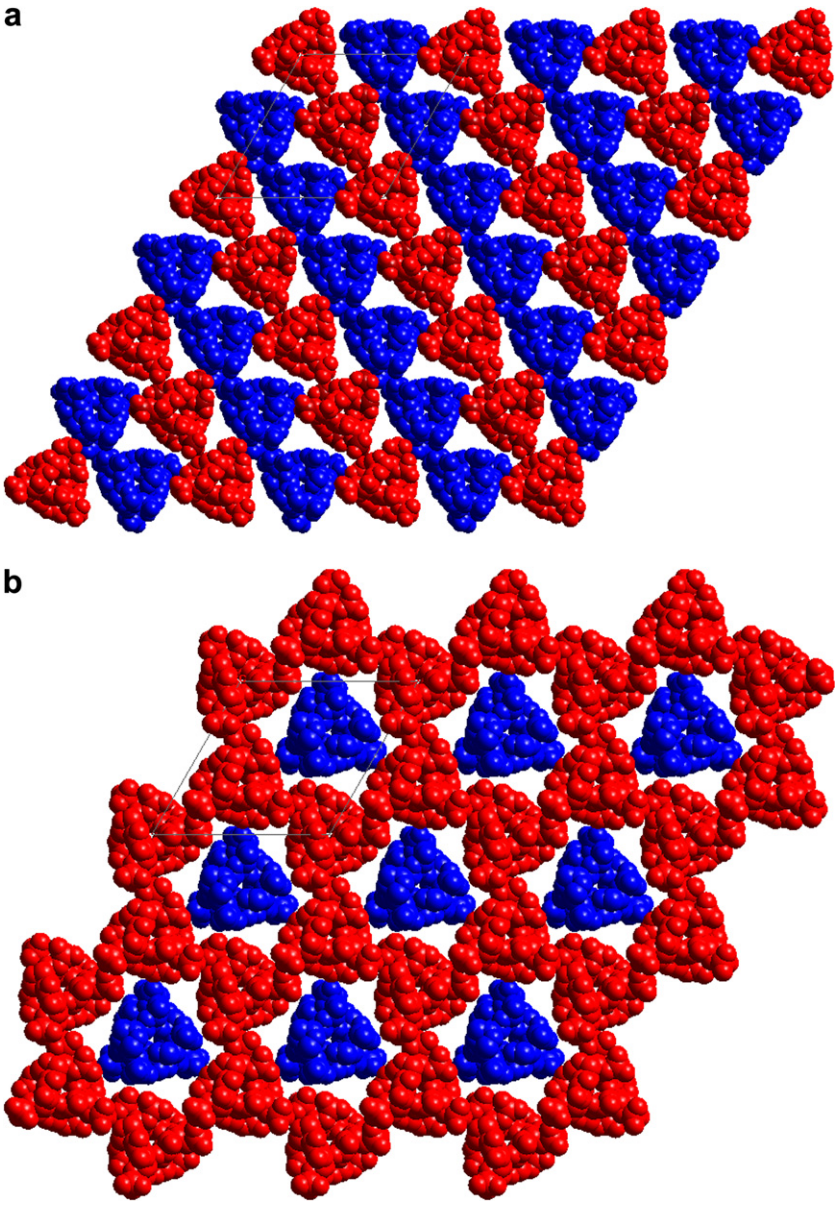

Figure 4. Space-filling models showing the association of ι-carrageenan helices, viewed down the *c*-axis, of (a) polymorph III compared with that of (b) polymorph II.[31] Color code: red for up-pointing and blue for down-pointing helix.

arrangement truly represent canonical B-DNA.[44] A pseudoorthogonal unit cell packing describes the structure of 10-fold poly (dA)·poly (dT).[45] These examples signify the ability of biopolymers in adapting variable morphology and packing mode for increasing their functionality.

4.2. Iota-carrageenan helices in motion

The effect of calcium ions in regulating polymorphs II and III is prima-facie obvious from their trigonal cell dimensions: a marginal decrease in the helix pitch (26.4 Å in II vs 26.02 Å III) and a substantial increase in the basal net dimensions (23.6 Å vs 27.44 Å). Consequently, consistent with fiber density, four helices are present in III compared to three in II. In both cases, adjacent helices are about 13.7 Å apart, referred as a_0 in the rest of the discussion. Space-filling models of helix axis projections for III and II are shown in Figure 4a and b, respectively. In the smaller unit cell of II, two up-pointing (U) and one down-pointing (D) helices are present and lined in an -U-U-D-U-U-D- sequence along the long diagonal (Fig. 4b) such that helices pointing the same way are arranged in sheets parallel to the $(\bar{1}10)$ plane. While the helices within a sheet are $\sqrt{3}a_0$ apart, the successive sheets are separated by $a_0/2$. The situation is quite different in III where helices are lined in -U-D-U-D- mode along the cell edges leading to a series of

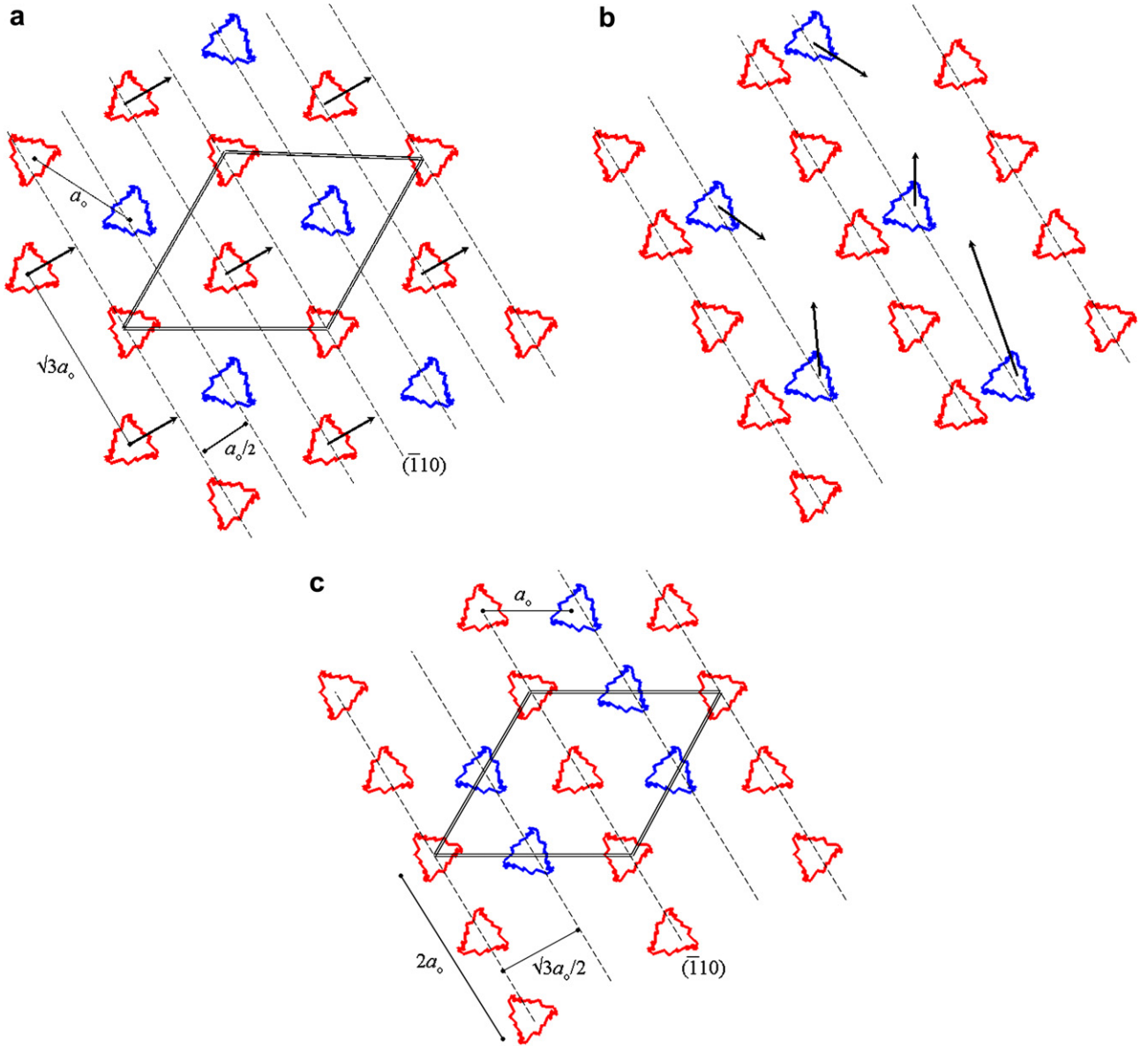

Figure 5. A snapshot of the rearrangement of ι-carrageenan helices from polymorph II leading to III, as viewed down the *c*-axis. (a) Polymorph II, (b) intermediate state of II→III and (c) polymorph III. The basal net of the trigonal cell is shown in double lines. Color code: red for up-pointing and blue for down-pointing helix. The dashed line represents a sheet. The arrow signifies the helix movement from a sheet.

rows of alternating up and down helices (Fig. 4a). This arrangement also leads to sheets of similar pointing helices along the short diagonal of the unit cell; however, the inter-helix separation in a sheet decreases to a_0 and inter-sheet gap increases to $\sqrt{3}a_0/2$.

A possible snapshot of the pathway from II to III is illustrated in Figure 5. As the up (↑) helices in II move from one sheet to the next, the initial interhelix distance $\sqrt{3}a_0$ in the sheet increases to $2a_0$ to accommodate the incoming neighbor (Fig. 5a). Thus after merger, adjacent up (↑) helices are uniformly spaced at a_0 within each newly formed sheet. In such a scenario, a large space is available for the down-pointing helices between the new sheets bestowing extra freedom to shuffle around (Fig. 5b). In the process of optimizing and strengthening the ensemble, the down (↓) helices move closer and reach the inter-helix distance of a_0. Simultaneously, the sheets also move relative to each other and close the gaps. This results in sheets of up-pointing and down-pointing helices (Fig. 5c) separated by $\sqrt{3}a_0/2$. Since any two adjacent helices (a_0 apart) in either U or D sheet are conformationally not the same, the most conservative unit cell will have two up-pointing and two down-pointing helices leading to polymorph III. The magic distance a_0 is preserved as the helices cannot come any closer due to strong electrostatic repulsion. Likewise, helices cannot be separated farther than a_0 as they will not be able to interact snugly through cations and water molecules toward junction zone formation.

The illustrated transition from II to III suggests that the polymer helices move around freely within the fiber. The soaking experiments involved in producing III from II might be responsible for this behavior as helices glide easily in the presence of excess water. Thus, the formation of III is more driven by helix movements. It is important to note that the population of down-pointing helices in III is less than in II. Consequently, the total number of unit cells in III is smaller than in II. This is consistent with the observation of relatively less crystalline diffraction pattern from III than from II. The ambient temperature seems to have a crucial role as II was observed at room temperature experiments whereas III at cold room temperature. During the rearrangement process, ι-carrageenan molecules rotate and translate about their helix axes and opportunistically bind ions and water molecules leading to a different set of interactions. Such helix movements explain the formation of cellulose III_I from cellulose I_β[46] as well as chitosan HI type I from hydrated chitosan.[47] To verify whether the II→III transition is reversible, further experiments are underway. Nevertheless, it is intriguing that ι-carrageenan has the ability to sustain its morphology and display highly crystalline diffraction patterns, and this intrinsic property bestows greater functional versatility than hitherto thought.

Acknowledgments

This work was supported by the Industrial Consortium of the Whistler Center for Carbohydrate Research. We thank Paul Chipman, Director, Electron Microscopy Facility, Structural Virology EM Studies, Department of Biology, Purdue University for scanning the diffraction patterns, and Professor I. Shomer for helpful discussions.

Supplementary data

Tables of (i) final atomic coordinates of the polysaccharide chain, calcium ions, and water molecules, (ii) observed and calculated structure factors and (iii) attractive interactions among the polysaccharide chains and water molecules. Supplementary data associated with this article can be found, in the online version, at doi:10.1016/j.carres.2007.10.020.

References

1. Potin, P.; Bouarab, K.; Salaün, J.; Pohnert, G.; Kloareg, B. *Curr. Opin. Plant Biol.* **2002**, *5*, 308–317.
2. Witvrouw, M.; DeClercq, E. *Gen. Pharmacol.* **1997**, *29*, 497–511.
3. Renn, D. *Trends Biotechnol.* **1997**, *15*, 9–14.
4. Zhou, G.; Sun, Y.; Xin, H.; Zhang, Y.; Li, Z.; Xu, Z. *Pharmacol. Res.* **2004**, *50*, 47–53.
5. Carlucci, M. J.; Ciancia, M.; Matulewicz, M. C.; Cerezo, A. S.; Damonte, E. B. *Antivir. Res.* **1999**, *43*, 93–102.
6. Farias, W. R. L.; Valente, A.; Pereira, M. S.; Mourão, P. A. S. *J. Biol. Chem.* **2000**, *275*, 29299–29307.
7. Yamada, T.; Ogamo, A.; Saito, T.; Uchiyama, H.; Nakagawa, Y. *Carbohydr. Polym.* **2000**, *41*, 115–120.
8. Smit, A. J. *J. Appl. Phycol.* **2004**, *16*, 245–262.
9. Therkelsen, G. H. In *Industrial gums. Polysaccharides and their derivatives*; Whistler, R. L., BeMiller, J. N., Eds.; Academic Press: New York, 1993; pp 145–180.
10. Piculell, L. In *Food Polysaccharides and their Applications*; Stephen, A. M., Ed.; Marcel Dekker: New York, 1995; pp 205–244.
11. Stortz, C. A.; Cerezo, A. S. *Curr. Top. Phytochem.* **2000**, *4*, 121–134.
12. Morris, E. R.; Rees, D. A.; Robinson, G. *J. Mol. Biol.* **1980**, *138*, 349–362.
13. Rochas, C.; Rinaudo, M. *Biopolymers* **1984**, *23*, 735–745.
14. Van de Velde, F.; Knutsen, S. H.; Usov, A. I.; Rollema, H. S.; Cerezo, A. S. *Trends Food Sci. Technol.* **2002**, *13*, 73–92.
15. Rochas, C.; Lahaye, M.; Yaphe, W. *Bot. Mar.* **1986**, *29*, 335–340.
16. Matsuhiro, B.; Rivas, P. *J. Appl. Phycol.* **1993**, *5*, 45–51.
17. Abeysekera, R. M.; Bergstrom, E. T.; Goodall, D. M.; Norton, I. T.; Robards, A. W. *Carbohydr. Res.* **1993**, *248*, 225–231.
18. Stokke, B. T.; Elgsaeter, A.; Kitamura, S. *Int. J. Biol. Macromol.* **1993**, *15*, 63–68.
19. Hjerde, T.; Smidsrod, O.; Christensen, B. E. *Biopolymers* **1999**, *49*, 71–80.

20. Bongaerts, K.; Paoletti, S.; Denef, B.; Vanneste, K.; Cuppo, F.; Reynaers, H. *Macromolecules* **2000**, *33*, 8709–8719.
21. Van de Velde, F.; Rollema, H. S.; Grinberg, N. V.; Burova, T. V.; Grinberg, V. Y.; Tromp, R. H. *Biopolymers* **2002**, *65*, 299–312.
22. Michel, A. S.; Mestdagh, M. M.; Axelos, M. A. V. *Int. J. Biol. Macromol.* **1997**, *21*, 195–200.
23. Pekcan, O.; Kara, S. *J. Biomater. Sci., Polym. Ed.* **2005**, *16*, 317–333.
24. Özbek, H.; Pekcan, O. *Physica A* **2006**, *367*, 69–78.
25. Hossain, K. S.; Miyanaga, K.; Maeda, H.; Nemoto, N. *Biomacromolecules* **2001**, *2*, 442–449.
26. Grinberg, V. Y.; Grinberg, N. V.; Usov, A. I.; Shusharina, N. P.; Khokhlov, A. R.; deKruif, K. G. *Biomacromolecules* **2001**, *2*, 864–873.
27. Arnott, S.; Scott, W. E.; Rees, D. A.; McNab, C. G. A. *J. Mol. Biol.* **1974**, *90*, 253–267.
28. Janaswamy, S.; Chandrasekaran, R. *Carbohydr. Polym.* **2005**, *60*, 499–505.
29. Janaswamy, S.; Chandrasekaran, R. *Macromolecules* **2006**, *39*, 3345–3349.
30. Janaswamy, S.; Chandrasekaran, R. *Carbohydr. Res.* **2001**, *335*, 181–194.
31. Janaswamy, S.; Chandrasekaran, R. *Carbohydr. Res.* **2002**, *337*, 523–535.
32. Rajkumar, G.; AL-Khayat, H. A.; Eakins, F.; He, A.; Knupp, C.; Squire, J. *Fiber Diff. Rev.* **2005**, *13*, 11–18.
33. Smith, P. J. C.; Arnott, S. *Acta Crystallogr., Sect. A* **1978**, *34*, 3–11.
34. Okada, K.; Noguchi, K.; Okuyama, K.; Arnott, S. *Comput. Biol. Chem.* **2003**, *27*, 265–285.
35. Hamilton, W. C. *Acta Crystallogr.* **1965**, *18*, 502–510.
36. Chuah, C. T.; Sarko, A.; Deslandes, Y.; Marchessault, R. H. *Macromolecules* **1983**, *16*, 1375–1382.
37. Deslandes, Y.; Marchessault, R. H.; Sarko, A. *Macromolecules* **1980**, *13*, 1466–1471.
38. Chandrasekaran, R. In *Advances in Carbohydrate Chemistry and Biochemistry*; Horton, D., Ed.; Academic Press: New York, 1997; pp 311–439.
39. Walkinshaw, M. D.; Arnott, S. *J. Mol. Biol.* **1981**, *153*, 1055–1073.
40. Okuyama, K.; Noguchi, K.; Kanenari, M.; Egawa, T.; Osawa, K.; Ogawa, K. *Carbohydr. Polym.* **2000**, *41*, 237–247.
41. Imberty, A.; Chanzy, H.; Perez, S.; Buleon, A.; Tran, V. *J. Mol. Biol.* **1988**, *201*, 365–378.
42. Takahashi, Y.; Kumano, T.; Nishikawa, S. *Macromolecules* **2004**, *37*, 6827–6832.
43. Chandrasekaran, R.; Wang, M.; He, R. G.; Puigjaner, L. C.; Byler, M. A.; Millane, R. P.; Arnott, S. *J. Biomol. Struct. Dyn.* **1989**, *6*, 1189–1202.
44. Chandrasekaran, R.; Arnott, S. *J. Biomol. Struct. Dyn.* **1996**, *13*, 1015–1027.
45. Chandrasekaran, R.; Radha, A.; Park, H. S.; Arnott, S. *J. Biomol. Struct. Dyn.* **1989**, *6*, 1203–1215.
46. Wada, M.; Chanzy, H.; Nishiyama, Y.; Langan, P. *Macromolecules* **2004**, *37*, 8548–8555.
47. Lertworasirikul, A.; Yokoyama, S.; Noguchi, K.; Ogawa, K.; Okuyama, K. *Carbohydr. Res.* **2004**, *339*, 825–833.